Tricritical behavior of polymers with loops

H. A. Lim
Supercomputer Computations Research Institute, Florida State University, Tallahassee, Florida 32306-4052

A. Guha* and Y. Shapir
Department of Physics and Astronomy, University of Rochester, Rochester, New York 14627-0011
(Received 8 September 1987; revised manuscript received 23 May 1988)

We study by exact enumerations a lattice model of polymers with fused loops (which also describes polymeric networks with even functional units). As the relative concentration of fused crossings of the chain (or that of the tetrafunctional units in the network) is increased, the conformations change their shapes from swollen (with self-avoiding-walk scaling properties) to compact. Earlier renormalization-group studies predicted the tricritical point associated with this transition to be in a new universality class, distinct from the Θ point. In particular, non-Gaussian behavior with $\nu_t < \frac{1}{2}$ and $\gamma_t < 1$ in three dimensions (3D) was predicted. We have enumerated all conformations according to their length l and number of crossings (or tetrafunctional units) I with their end-to-end distance r, on triangular (up to $l=15$, $I=7$), square ($l=21$, $I=7$), and cubic ($l=15$, $I=5$) lattices. The locations of their respective transitions are determined from the divergence of the specific-heat plots. Tricritical couplings and exponents are extracted by a D log Padé analysis. The tricritical scaling exponents we find are $\nu_t \simeq 0.52(2)$, $\gamma_t \simeq 1.25(20)$ in 2D, and $\nu_t \simeq 0.465(10)$, $\gamma_t \simeq 0.60(5)$ in 3D, in fair agreement with the renormalization-group predictions.

I. INTRODUCTION

In a series of recent papers,[1-4] we have initiated the investigations of new tricritical points describing collapse transitions in models of intersecting walks, polymers with loops, and polymeric networks with even-functional units. We have considered two basic models depicted in Fig. 1: (i) trails [Fig. 1(a)] and (ii) their silhouettes [Fig. 1(b)]. Trails[2-6] are paths followed by a walker allowed to step at most once on each bond but which may self-cross its path through an already visited site. The second model is that of the silhouettes or shadows of the trails. Note that a silhouette may have many trails [e.g., there are six different trails corresponding to the silhouette in Fig. 1(b)]. The problem of their enumeration goes back to Euler, who fathered graph theory.

By assigning a fugacity $f=\exp\theta$ to each crossing, we have a handle over their average concentration ($E=-k_BT\theta$ may be thought of as the energy gained by the formation of the crossing). In Ref. 2 and 3, we have presented and analyzed the scaling behavior of the trail model [Fig. 1(a)]. In the present work, we follow a parallel investigation of the silhouettes [Fig. 1(b)]. Their enumeration presents a computational challenge to a certain degree. The computational complexities and the technical details of their resolution will be discussed elsewhere. The motivation for studying silhouettes are twofold: Firstly, it is a model of its own interest within the realm of statistical mechanics, since it exhibits new scaling (fractal) behavior with its own universal exponents; secondly, this model describes polymers with fused loops. Moreover, if the two ends of the polymer are forced to join (and close the path), the same model describes polymeric network with even-functional vertices. We note, in passing, that only one crossing (or tetrafunctional unit) is important. Whether double (or more) crossings, which may occur if the coordination number is larger than four (or hexafunctionals, octafunctionals, etc.), are allowed or not is "irrelevant" in the renormalization-group (RG) sense.

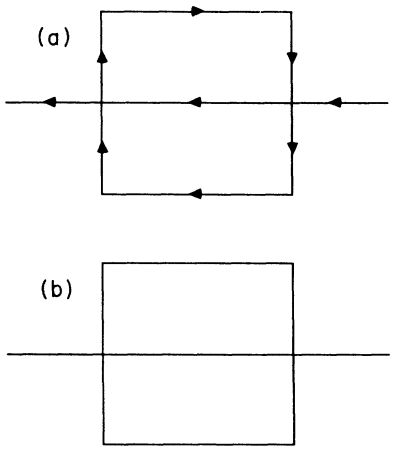

FIG. 1. (a) A directed graph that may be traced by two different trail configurations; (b) the silhouette of these trails. Note that six different trails have this same silhouette: The other four correspond pairwise to two other directed graphs.

Concentrating on the silhouette model [Fig. 1(b)], all previous results on their scaling behavior were derived using the RG approach with an $\sqrt{\epsilon}$ expansion[4] ($\epsilon=4-d$). These calculations were based on the "magnetic analog" Hamiltonian for the generating functions of the configurations.[1] Before proceeding to describe the new results derived by exact enumerations, we summarize the RG results.[4] If was found[4] that as the average density of crossings (or of tetrafunctional units) is varied, three regimes are encountered: A swollen phase with the scaling exponents of self-avoiding walks (SAW) for small concentrations, a collapsed phase (with the shape exponent $\nu=1/d$) for large concentrations, and a tricritical regime at a critical concentration (or fugacity) which separates these first two regimes. Our study focuses on this tricritical regime. The situation is very similar to that which takes place at the Flory Θ point of linear polymer in poor solvents[7] or of a SAW with nearest-neighbor attractions.[8] The upper critical dimension of the Θ point is $d^*=3$ and the conformations in three dimensions (3D) are Gaussians (up to logarithmic corrections).[8-15] The tricritical points due to increasing the crossing concentration in the silhouette model is in another universality class: In particular, its upper critical dimension is $d^*=4$ and the 3D configurations are predicted to be non-Gaussian.[4] This tricritical point is of order $\sqrt{\epsilon}$ in $d=4-\epsilon$ dimensions[1] and the expansion in $\sqrt{\epsilon}$ for the scaling exponents to second order (ϵ) are[4] (a remainder of their definition is given in Sec. II):

$$\gamma_t(\epsilon)=1-\frac{1}{2}\left[\frac{6}{53}\right]^{1/2}\epsilon^{1/2}+\frac{1}{4}\left[\frac{429-756\zeta(3)}{5618}\right]\epsilon\ , \tag{1.1}$$

where $\zeta(3)=1.202\,06$ is the Euler ζ function, subscript t denotes "tricritical" and

$$\nu_t(\epsilon)=\frac{1}{2}\left[1-\frac{1}{2}\left[\frac{6}{53}\right]^{1/2}\epsilon^{1/2}+\frac{1}{2}\left[\frac{535-756\zeta(3)}{5618}\right]\epsilon\right]\ , \tag{1.2}$$

which may also be approximated by the [1/1] Padé:

$$\nu_t(\epsilon)=\frac{1}{2}\left[\frac{1+0.117\epsilon^{1/2}}{1+0.285\epsilon^{1/2}}\right]\ . \tag{1.3}$$

Inserting $\epsilon=1$ in Eqs. (1.1) (1.2), we find in 3D

$$\gamma_t(1)=0.81\ , \tag{1.4}$$

$$\nu_t(1)=0.40\ , \tag{1.5}$$

or from Eq. (1.3),

$$\nu_t(1)=0.435\ . \tag{1.6}$$

The most striking fact about these results are the unusual deviations from the mean-field exponents to lower values ($\gamma_t<1$ and $\nu_t<\frac{1}{2}$) in 3D. We anticipate $\nu=1/d$ in the collapsed phase, $\nu_t>\frac{1}{3}$ (and $\nu_t>\frac{1}{2}$) at the 3D (2D) tricritical points. So the trend for smaller exponents below $d^*=4$ should reverse itself at a lower dimension for ν_t to satisfy the 2D bound and the exponents are expected to be monotonic function of the dimensionality.

To check all these predictions, we have decided to analyze this collapse transition by exact enumerations of silhouettes on 2D and 3D lattices. The results of these extensive enumerations are presented in this paper which is organized as follows: In the next section (Sec. II), the basic definitions of the different statistical functions, their relations, and the scaling exponents describing their asymptotic behaviors, are given. The results for the different lattices: triangular, square, and cubic are presented in Secs. III, IV, and V, respectively. The last section (Sec. VI) is devoted to discussions and conclusions.

II. DEFINITIONS AND SYMBOLS

Throughout the paper, the following notations are used: l denotes the total number of monomers in the polymer (proportional to its molecular mass), I denotes the number of tetrafunctional units (crossings) in the network configurations, r denotes the end-to-end distance of the two free ends we associate with each configuration [Fig. 1(b)].

For each of the lattices, we have enumerated $n(l,I,r)$ as the total number of polymer configurations [Fig. 1(b)] with length l, I crossings, and end-to-end distance r. From them we have generated the following series: (a) $c(l,I)=\sum_r n(l,I,r)$—the total number of silhouettes of length l with I crossings (namely tetrafunctional units) and (b) $d(l,r)=\sum_r r^2 n(l,I,r)$—which is the average square end-to-end distance (see below).

In order to control the average number of crossings (tetrafunctional units), we introduce a fugacity $f=\exp(\theta)$ ($\theta=-E/k_BT$, where E is the energy gained by the cross linking) per such crossing. Using the coefficient $c(l,I)$, the weighted series $U_l(\theta)$ are derived

$$U_l(\theta)=\sum_{I\geq 0} c(l,I)e^{I\theta}\ . \tag{2.1}$$

The average square end-to-end distance will be derived from the following ratio:

$$\langle r_l^2(\theta)\rangle=\sum_{I\geq 0}\frac{d(l,I)e^{I\theta}}{U_l(\theta)}\ . \tag{2.2}$$

The critical exponents are related to their behavior as $l\to\infty$:[8]

$$U_l(\theta)\to\Gamma(\theta)l^{\gamma(\theta)-1}\mu^l(\theta)\ , \tag{2.3}$$

$$\langle r_l^2(\theta)\rangle\to B(\theta)l^{2\nu(\theta)}\ . \tag{2.4}$$

The amplitudes $\Gamma(\theta)$ and $B(\theta)$ as well as the effective "growth parameter" $\mu(\theta)$ are nonuniversal quantities. The critical exponents $\gamma(\theta)$ and $\nu(\theta)$, however, are universal and are expected to assume only three possible values: (a) $\nu=\nu_{\rm SAW}$, $\gamma=\gamma_{\rm SAW}$ for $\theta<\theta_t$ in swollen phase; (b) $\nu=\nu_t$, $\gamma=\gamma_t$ at the tricritical point $\theta=\theta_t$; or (c) $\nu=1/d$, $\gamma=\gamma_c$ in the dense phase $\theta>\theta_t$.

TABLE I. The coefficients $c(l,I)/6$ for the triangular lattice.

	$\frac{1}{6}c(l,I)$							
l/i	0	1	2	3	4	5	6	7
1	1							
2	5							
3	23	1						
4	103	10						
5	455	67	1					
6	1991	383	$17\frac{1}{2}$					
7	8647	2035	163	2				
8	373 55	10 336	1163	34				
9	160 689	50 972	7207	$372\frac{1}{3}$	4			
10	688 861	245 916	41 307	3128	81			
11	2 944 823	1 166 693	225 075	22 222	956	6		
12	12 559 201	5 462 666	$1\,183\,576\frac{1}{2}$	$141\,984\frac{1}{3}$	8669	168		
13	53 455 781	25 304 232	6 060 900	846 335	67 164	2328	13	
14	227 131 875	116 178 379	$30\,397\,994\frac{1}{2}$	4 806 492	$465\,757\frac{1}{2}$	23 532	$357\frac{1}{2}$	
15	963 627 597	529 425 453	149 935 192	$26\,336\,716\frac{2}{3}$	2 985 233	197 528	5481	33

In order to find the tricritical value θ_t of the controlling parameter θ, we shall explore the behavior of the specific heat defined as follows:

$$h_l(\theta)=l^{-1}\frac{\partial^2}{\partial\theta^2}\ln U_l(\theta)\,, \tag{2.5}$$

$$=\langle I^2(\theta)\rangle-\langle I(\theta)\rangle^2\,, \tag{2.6}$$

which measures the relative fluctuations in the number of crossings. Rapaport first suggested,[12] in the context of the Θ point of SAW, to look for the specific heat divergence (as a function l) as the signature for the tricritical point.

III. TRIANGULAR LATTICE ENUMERATIONS

A. Tabulation

The enumerations of the series $c(l,I)/6$ and $d(l,I)/6$ for the triangular lattice up to $l=15$ and $I=7$ are presented in Tables I and II, respectively.

B. Specific heat

The specific-heat plots $h_l(\theta)$ for $l=11-15$ are depicted in Fig. 2. The plot with $l=11$ is the lowest one and, as expected, their relative heights increase with l. We find a regular shift of the values of $\theta=\theta_{\max}(l)$ corresponding to

TABLE II. The coefficients $d(l,I)/6$ for the triangular lattice.

	$\frac{1}{6}d(l,I)$							
l/I	0	1	2	3	4	5	6	7
1	1							
2	12							
3	97							
4	654	8						
5	3977	132	1					
6	22 624	1344	24					
7	122 821	10 908	351	2				
8	644 082	77 446	3818	58				
9	3 288 739	503 246	34 169	894	6			
10	16 440 648	3 069 972	267 736	10 328	166			
11	80 783 857	17 861 068	1 908 555	99 484	2652	12		
12	391 310 240	100 152 740	12 681 386	841 712	315 82	392		
13	1 872 763 387	545 238 848	79 824 910	6 463 020	314 142	6882	31	
14	8 870 963 422	2 897 323 704	481 385 766	46 061 078	2 760 472	88 622	1016	
15	41 647 686 501	15 088 036 614	2 803 780 558	309 542 172	22 111 099	938 580	18 597	72

the maxima of $h_l(\theta)$ as l increases. We therefore improve the estimate by a linear approximation: in Fig. 3, $\theta_{\max}(l)$ are plotted versus $1/l$. The linear intercept with the $1/l=0$ yields our estimate for the tricritical point θ_t. Although higher-order and noninteger powers (related to the crossover exponent ϕ) of $1/l$ are certainly present, the linear approximation provides a substantial improvement over the choice of the highest maxima at the tricritical location. Using Fig. 3, we predict

$$\theta_t^{\rm tr}\approx 1.60\pm 0.05 \ . \tag{3.1}$$

C. *D* log Padé analysis

To extract the tricritical values μ_t and γ_t from the asymptotic behavior of $U_l(\theta)$ [Eq. (2.3)], we apply the standard *D* log Padé method to the series. In Table III, values of μ_t and γ_t for $\theta=1.6$ (the extrapolated value) and also for later comparisons, for $\theta=1.7$, 1.8, and 1.9 (the latter being the location of the last, highest maximum). We observe that [6/7] has only defective poles. Interferences of nonphysical poles also harm the results from [7/6] and [7/7]. Based on the values from other approximants at $\theta_t=1.6$, we estimate

$$\gamma_t^{\rm tr}=1.4\pm 0.1 \ , \tag{3.2}$$

$$\mu_t^{\rm tr}=5.07\pm 0.25 \ . \tag{3.3}$$

We note that had we chosen the highest maxima $\theta=1.9$ (without extrapolation), the value of γ_t would have been smaller ($\gamma_t\sim 1.25-1.3$) and μ_t larger ($\mu_t\sim 5.45-5.50$). The value of ν_t is extracted from $\langle r_l^2(\theta)\rangle$ in Eq. (2.4). This series diverges and has one as the critical point. The exponent ν_t must be larger than $\frac{1}{2}$ which is the lower bound (expected only in the dense phase.) The value of ν_t (in parentheses the "critical point" which should be exactly one) for $\theta=1.6$ from the highest approximants are [5/6], 0.495(1.010); [6/5], 0.480(1.012); [6/6], 0.495(1.010); [6/7], 0.495(1.010); [7/6], 0.520(1.008); and [7/7], 0.516(1.008). Because the lower limit is 0.5, only the last two values are physically possible, and we choose as our best estimate the [7/7] result:

$$\nu_t=0.516\pm 0.16 \ . \tag{3.4}$$

For higher values of θ, 1.7–1.9, we find even smaller values of ν_t (smaller than 0.5 for [7/7] as well). We suspect that the problems manifested in $U_l(\theta)$ by the many spurious poles in Table III also alter the behavior of $\langle r_l^2(\theta)\rangle$ to give incorrectly small values of ν_t. An alternative method to compute this exponent is discussed in the next section.

D. Generalized ratio method

In a recent analysis of the Θ point, Privman introduced an extension of the ratio method which gives with improved accuracy both the location and the value ν_t of the tricritical point.[14] They are extracted from the recursive estimates

$$\nu_l=\frac{1}{2}\frac{\ln\dfrac{r_l^2}{r_{l-1}^2}}{\ln\dfrac{l}{l-1}} \ , \tag{3.5}$$

and the deviation from the average ν

$$\delta\nu_l=\nu_l-\frac{1}{m}\sum_{k=n+1}^{n+m}\nu_k \ . \tag{3.6}$$

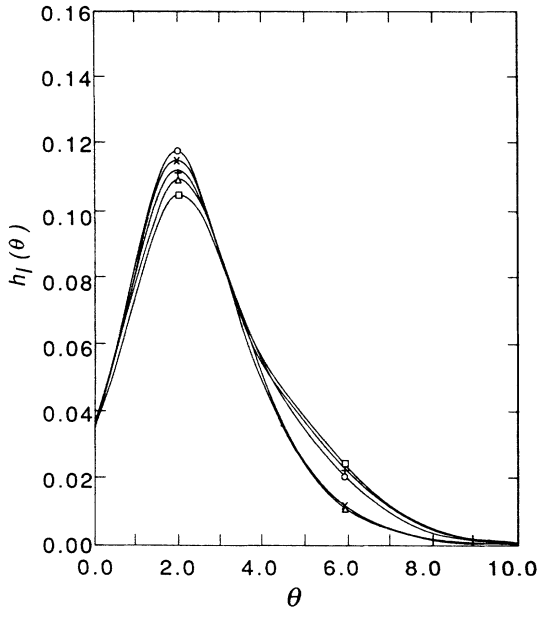

FIG. 2. Specific-heat plots $h_l(\theta)$ for $l=11-15$ for the triangular lattice.

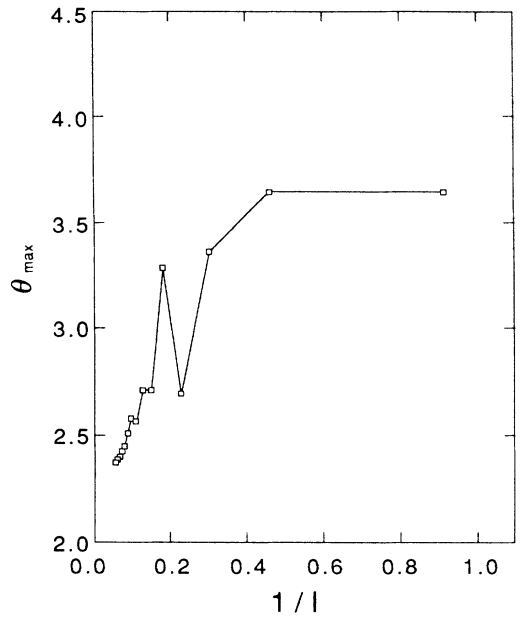

FIG. 3. The specific-heat maxima $\theta_{\max}(l)$ (from Fig. 2) vs $1/l$, for the triangular lattice.

TABLE III. γ_t (μ_t) vs θ between $\theta_{max}(l=15)=1.9$ and θ_{max} (extrapolated)$=1.6$ for the triangular lattice. $\times$ indicates defective poles.

	γ_t (μ_t)			
$[L/M]/\theta$	1.6	1.7	1.8	1.9
[5/6]	1.403	1.368	1.326	1.285
	(5.076)	(5.193)	(5.322)	(5.464)
[6/5]	1.398	1.359	1.309	1.252
	(5.077)	(5.195)	(5.327)	(5.473)
[6/6]	1.425	1.400	1.374	1.356
	(5.071)	(5.185)	(5.311)	(5.449)
[6/7]	$\times$	$\times$	$\times$	$\times$
	($\times$)	($\times$)	($\times$)	($\times$)
[7/6]	1.545	1.564	1.610	1.738
	(5.050)	(5.158)	(5.276)	(5.400)
[7/7]	1.544	1.546	1.540	1.537
	(5.050)	(5.161)	(5.284)	(5.420)

In Figs. 4 and 5, we plot ν_l and $\delta\nu_l$, respectively, for $l=11-15$ ($n=10$, $m=5$). The tricritical point is supposed to be at the point of minimal spread in $\delta\nu$. If we include all $\delta\nu$, the minimal spread is at $\theta_{min}=2.1$, and if $\delta\nu_l$ for $l=12-15$ are included, the minimal spread is at $\theta_{min}=1.9$. This last value coincides with the last maximum in the specific heat but does not account for the steady trend of the shift in θ_t (and which is accounted for by the linear extrapolation). The difference between the values of θ at the minimal spread, with ($\theta_{min}=2.1$) and without ($\theta_{min}=1.9$) the $\delta\nu_{11}$ term, indicates that a steady shift in θ_{min} in the Privman's method is likely to take place. The value of ν at $\theta_{min}=1.9$ is in perfect agreement with the Padé result at that value of θ, namely $\nu_t \approx 0.48$. As the shift implies a smaller asymptotic value for θ_{min}, larger values of $\nu_t(>\frac{1}{2})$ will also be obtained. Since we do not have enough terms to actually calculate a quantitative estimate for the shift, we are also limited in our possibility to use this method to get reliable values for the exponent ν_t. The results of this section will be discussed and compared with those of the square lattice (next section) in the last section (Sec. VI).

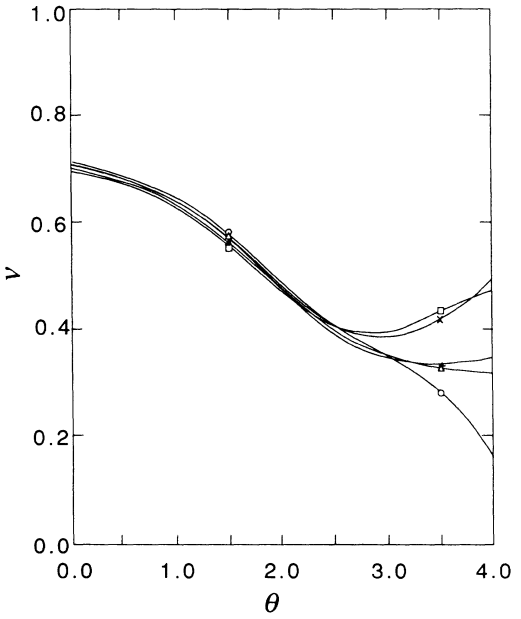

FIG. 4. The exponents $\nu_l(\theta)$ ($l=11-15$) from the generalized ratio method [Eq. 3.5)], for the triangular lattice.

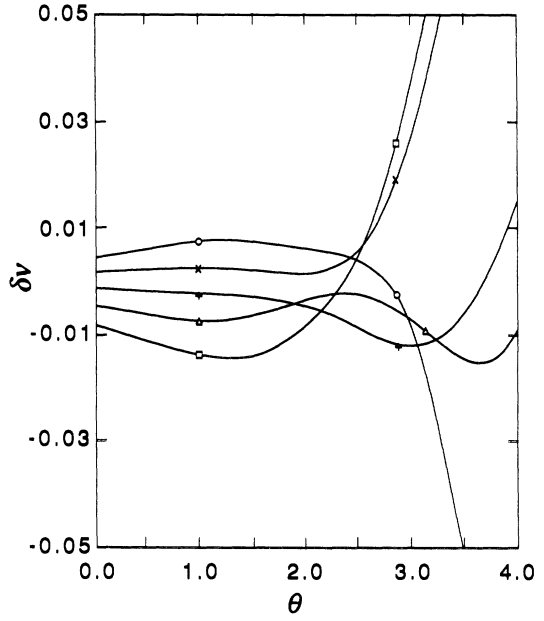

FIG. 5. The values of $\delta\nu_l(\theta)$ ($l=11-15$) extracted from ν_l in Fig. 4 using Eq. (3.6), for the triangular lattice.

TABLE IV. The coefficients $c(l,I)/4$ for the square lattice.

	$\frac{1}{4}c(l,I)$							
l/I	0	1	2	3	4	5	6	7
1	1							
2	3							
3	9							
4	25	1						
5	71	4						
6	195	17						
7	543	54	1					
8	1479	184	5.5					
9	4067	554	29					
10	11 025	1738	105	2				
11	30 073	5128	394	8				
12	81 233	15 380	1323	53				
13	220 375	44 702	4364	208	4			
14	593 611	130 704	14 069	830	18			
15	1 604 149	375 216	43 961	3024	99			
16	4 311 333	1 079 572	136 928	10 476	446.5	9		
17	11 616 669	3 068 788	416 130	35 492	1764	48		
18	31 164 683	8 729 776	1 263 268	116 744	6874	234	2	
19	83 779 155	24 623 430	3 768 812	376 284	24 807	1040	16	
20	224 424 291	69 449 248	11 233 384	1 198 294	87 142	4270	130	
21	602 201 507	194 666 934	33 052 280	3 746 540	297 832	16 250	587	8

IV. SQUARE-LATTICE ENUMERATIONS

A. Tabulation

The series $c(l,I)/4$ and $d(l,I)/4$ for the square lattice up to $l=21$ and $I=7$ are presented in Tables IV and V, respectively. (They took about 100 CPU hours on a VAX8600 to enumerate.)

B. Specific heat

The specific-heat plots $h_l(\theta)$ for $l=11-21$ for the square lattice are plotted in Fig. 6 with $l=11$ being the lowest and $l=21$ the highest in ascending order. We again observe the same trend of shift in the maxima discussed in Sec. III B. Here, however, there are also super-

TABLE V. The coefficients $d(l,I)/4$ for the square lattice.

	$\frac{1}{4}d(l,I)$							
l/I	0	1	2	3	4	5	6	7
1	1							
2	8							
3	41							
4	176							
5	679	4						
6	2452	36						
7	8447	214	1					
8	28 120	1048	8					
9	91 147	4538	69					
10	289 324	18 188	400	4				
11	902 721	68 792	2098	24				
12	2 777 112	249 336	9616	176				
13	8 441 319	873 774	41 100	944	12			
14	25 398 500	2 980 300	165 016	4848	68			
15	75 744 301	9 941 824	633 289	22 544	475			
16	224 156 984	32 551 736	2 342 232	98 136	2464	32		
17	658 855 781	104 905 092	8 408 186	406 100	12 260	192		
18	1 924 932 324	333 500 620	29 434 872	1 606 188	56 596	1280	4	
19	5 593 580 859	1 047 696 230	100 908 548	6 134 956	247 399	6720	96	
20	16 175 728 584	3 257 208 608	339 692 960	22 739 320	1 031 936	33 000	608	
21	46 572 304 083	10 033 256 694	1 125 821 936	82 180 844	4 150 920	150 986	3691	24

imposed oscillations due to the interference of the "antiferromagnetic singularity," typical of "two sublattices" lattices, and which were not present in the case of the close-packed triangular lattice. Therefore our method to extrapolate $\theta_{\max}(l)$ versus $1/l$ to $1/l=0$ (depicted in Fig. 7) is not as efficient here to determine θ_t, as it was for the triangular lattice. Based on this plot, we estimate $\theta_t^{\rm sq}\sim 2.45-2.49$.

C. *D* log Padé analysis

The extrapolated value of $\theta_t^{\rm sq}$ is between $\theta=2.45$ and 2.49. For values of θ in this range, we present in Table VI the results for γ_t (and μ_t). We choose to show the results from the highest possible diagonal $[M/M]$, and off-diagonal $[(M-1)/M]$ and $[M/(M-1)]$ Padé approximants. Defective poles are denoted by crosses. We note the good convergence of the result for θ_t around 2.8 (except for [10/9] which deviates slightly). This leads us to the following estimates:

$$\gamma_t^{\rm sq}=1.250\pm 0.006\ , \tag{4.1}$$

$$\mu_t^{\rm sq}=3.24\pm 0.01\ . \tag{4.2}$$

The series for $\langle r_l^2(\theta)\rangle$ do not follow such a coherent behavior. The approximants [9/10] and [10/9] yield only spurious poles. The results for ν_t (and for μ_t; the "location" of the critical point should be $\mu_t\equiv 1$) from the other approximants are presented in Table VII. Since $\nu_t^{\rm sq}=\frac{1}{2}$ is a lower limit, we give more credibility to the results of [8/9] and [10/10] from which we conclude the estimates

$$\nu_t^{\rm sq}=0.53\pm 0.03\ . \tag{4.3}$$

In Sec. VI, these results will be discussed and compared with the estimates extracted in the previous section for the triangular lattice.

V. CUBIC LATTICE ENUMERATION

A. Tabulation

The coefficients $c(l,I)/6$ and $d(l,I)/6$ for the cubic lattice with $l=1-15$ and $I=0-5$ are tabulated in Tables VIII and IX.

B. Specific heat

The specific-heat plots $h_l(\theta)$ with $l=11-15$ are plotted in Fig. 8. Again, the lowest plot corresponds to $l=11$, the next 12, and so on up to the highest with $l=15$. The plot of the locations of their respective maxima $\theta_{\max}(l)$ versus $1/l$ is shown in Fig. 9. Based on the extrapolation to $1/l=0$, we estimate the tricritical point to be in the range $\theta_t^c\sim 2.5-2.8$.

C. *D* log Padé analysis

The extrapolated θ_t^c for the simple cubic lattice from the specific-heat maxima is between 2.5 and 2.8. We therefore present (Table X) the results for γ_t^c and μ_t^c as derived from the highest diagonal and off-diagonal approximants for this range of values of θ. The figures from [6/7] and [7/7] deviate due to the presence of another pole not far from the physical one. However, that may also be an indication for a crossover to another behavior at large l. We still choose to base our estimates on the behavior of the other approximants for $\theta\sim 2.6-2.7$. Our best estimates are

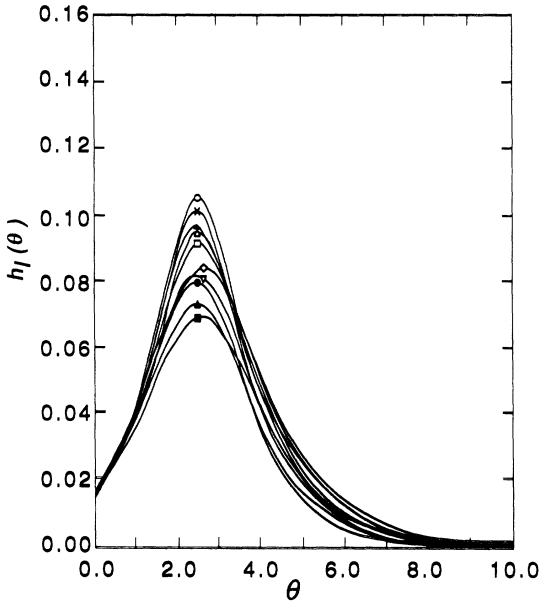

FIG. 6. Specific heat $h_l(\theta)$, $l=11-21$ for the square lattice.

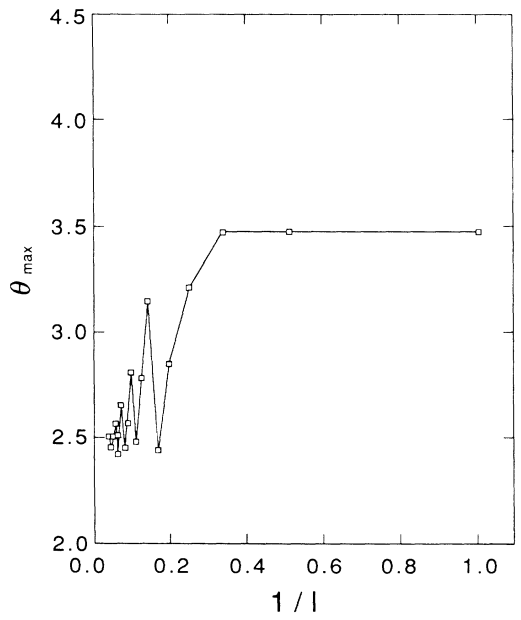

FIG. 7. $h_l(\theta)$ vs $1/l$ for the square lattice.

TABLE VI. The exponents γ_t^{sq} and the growth parameter μ_t^{sq} for different values of θ on the square lattice.

	γ_t (μ_t)				
$[L/M]\theta$	2.45	2.46	2.47	2.48	2.49
[8/9]	1.269	×	1.258	1.252	1.246
	(3.217)	(×)	(3.232)	(3.239)	(3.247)
[9/8]	1.261	1.261	1.256	1.251	1.246
	(3.221)	(3.226)	(3.232)	(3.239)	(3.246)
[9/9]	1.257	1.258	1.254	1.250	1.246
	(3.224)	(3.227)	(3.234)	(3.240)	(3.246)
[9/10]	1.257	1.254	1.251	1.247	1.244
	(3.221)	(3.230)	(3.236)	(3.242)	(3.248)
[10/9]	1.250	1.247	1.243	1.239	1.235
	(3.228)	(3.234)	(3.240)	(3.247)	(3.253)
[10/10]	1.265	1.261	1.256	1.252	1.247
	(3.198)	(3.203)	(3.208)	(3.213)	(3.253)

TABLE VII. The exponents ν_t^{sq} (and the critical coupling $\mu_t^{sq} \equiv 1$) in the vicinity of θ_t^{sq} of the square lattice.

	ν_t (μ_t)				
$[L/M]/\theta$	2.45	2.46	2.47	2.48	2.49
[8/9]	0.550	0.478	0.553	0.555	0.557
	(0.996)	(1.002)	(0.995)	(0.995)	(0.994)
[9/8]	0.498	0.552	0.452	0.495	0.494
	(1.000)	(0.995)	(1.007)	(0.999)	(0.999)
[9/9]	0.456	0.497	0.788	0.450	0.448
	(1.006)	(1.000)	(1.041)	(1.007)	(1.007)
[10/10]	0.551	0.547	0.543	0.539	0.535
	(0.994)	(0.994)	(0.994)	(0.994)	(0.994)

TABLE VIII. The coefficients $c(l,I)/6$ for the simple cubic lattice.

	$\frac{1}{6}c(l,I)$					
l/I	0	1	2	3	4	5
1	1					
2	5					
3	25					
4	121	2				
5	589	16				
6	2821	126				
7	13 565	780	6			
8	64 661	4784	79			
9	308 981	27 100	$720\frac{2}{3}$			
10	1 468 313	152 148	5612	44		
11	6 989 025	823 488	38 288	528		
12	33 140 457	4 423 380	249 501	$5664\frac{1}{3}$	16	
13	157 329 085	23 281 204	1 523 630	45 806	381	
14	744 818 613	121 767 700	9 116 706	351 106	5164	4
15	3 529 191 009	628 827 480	$52\,529\,729\frac{1}{3}$	24 049 62	51 143	216

TABLE IX. The coefficients $d(l,I)/6$ for the simple cubic lattice.

	$\frac{1}{6}d(l,I)$					
l/I	0	1	2	3	4	5
1	1					
2	12					
3	97					
4	672					
5	4261	16				
6	25 588	248				
7	147 821	2604	6			
8	830 576	22 240	112			
9	4 566 917	168 828	1638			
10	24 692 980	1 182 200	17 656	56		
11	131 682 825	7 820 704	164 640	1104		
12	694 386 864	49 547 760	1 360 944	14 992	32	
13	3 626 770 709	303 596 852	10 404 126	163 566	941	
14	18 790 632 772	1 810 823 512	74 651 504	1 543 336	14 264	16
15	96 675 376 705	10 566 185 208	511 052 492	13 227 474	176 911	536

$$\gamma_t^c = 0.60 \pm 0.05 \ , \tag{5.1}$$

$$\mu_t^c = 6.05 \pm 0.15 \ . \tag{5.2}$$

In Table XI, the results for ν_t^c (and the critical value μ_t^c which is supposed to be precisely unity) are given for the same range of θ and the same approximants. From these best-behaved approximants we estimate

$$\nu_t^c = 0.465 \pm 0.010 \ . \tag{5.3}$$

VI. DISCUSSION AND CONCLUSIONS

The results we obtain for the simple cubic lattice $\nu_t^c \approx 0.465$, $\gamma_t^c \approx 0.60$ agree quite well with the rough predictions[4] of the RG $\sqrt{\epsilon}$ expansion extrapolated to $\epsilon = 1$: $\nu_t \approx 0.435$ and $\gamma_t \approx 0.81$. Most importantly, the unusual values of $\gamma_t < 1$ and $\nu_t < \frac{1}{2}$ are confirmed by our series. This lends strong support for the existence of a new universality class for the tricritical behavior at the collapse transition of evenfunctional networks. It will be ex-

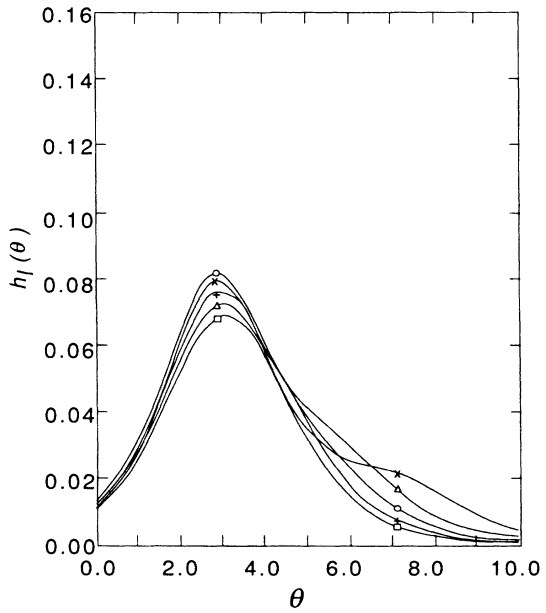

FIG. 8. Specific heat $h_l(\theta)$, $l = 11-15$ for the simple cubic lattice.

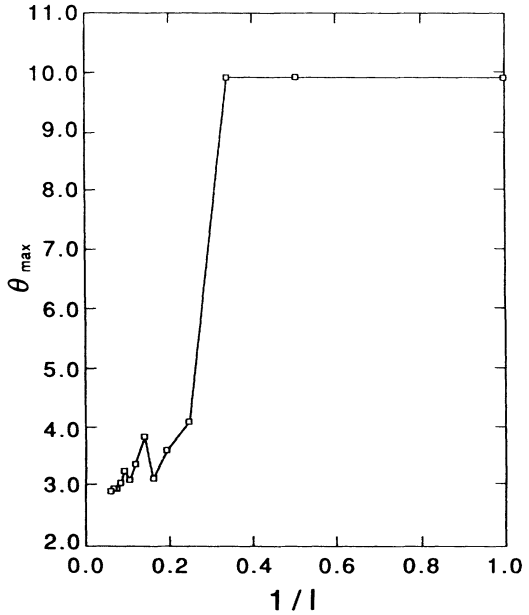

FIG. 9. $h_l(\theta)$ vs $1/l$ for the simple cubic lattice.

TABLE X. The exponent γ_t^c and the growth parameter μ_t^c in the vicinity of θ_t^c of the cubic lattice.

	γ_t (μ_t)			
$[L/M]/\theta$	2.5	2.6	2.7	2.8
[5/6]	0.756	0.717	0.678	0.639
	(5.77)	(5.88)	(6.00)	(6.14)
[6/5]	0.691	0.643	0.594	0.546
	(5.81)	(5.94)	(6.07)	(6.22)
[6/6]	0.708	0.660	0.610	0.562
	(5.80)	(5.93)	(6.06)	(6.21)
[6/7]	0.620	0.573	0.529	0.488
	(5.86)	(5.98)	(6.12)	(6.27)
[7/6]	0.697	0.648	0.599	0.551
	(5.81)	(5.93)	(6.07)	(6.22)
[7/7]	0.611	0.541	0.467	0.381
	(5.86)	(6.00)	(6.16)	(6.35)

TABLE XI. The exponent ν_t^c (and the critical coupling $\mu_t^c \equiv 1$) in the vicinity of θ_t^c of the cubic lattice.

	ν_t (μ_t)			
$[L/M]/\theta$	2.5	2.6	2.7	2.8
[5/6]	0.452	0.448	0.443	0.438
	(0.99)	(0.98)	(0.98)	(0.98)
[6/5]	×	×	×	×
	(×)	(×)	(×)	(×)
[6/6]	0.477	0.476	0.474	0.472
	(0.98)	(0.98)	(0.98)	(0.97)
[6/7]	0.466	0.463	0.459	0.456
	(0.98)	(0.98)	(0.98)	(0.98)
[7/6]	0.457	0.453	0.448	0.443
	(0.99)	(0.98)	(0.98)	(0.98)
[7/7]	0.490	0.492	0.493	0.493
	(0.98)	(0.98)	(0.97)	(0.97)

tremely interesting to try to control the number of tetrafunctional units in addition polymerization reactions and actually observe this new scaling behavior experimentally.

In 2D, the series for the square lattice exhibit a more regular behavior than the triangular ones (despite the interference from the "antiferromagnetic" singularity). We therefore give more credibility to the square lattice results over those of the triangular lattice. Since we expect the exponent η_t defined by $(2-\eta_t)\nu_t=\gamma_t$ to be nonnegative, the asymptotic values of ν_t (and/or γ_t) in 2D will be somewhat larger (smaller) than our present estimates. For comparison, the best estimate we have used for trails are $\nu_t=0.48(3)$, $\gamma_t=0.43(6)$ in 3D and $\nu_t=0.52(2)$, $\gamma_t=1.18(4)$ in 2D.

Although our series provide support for the RG predictions for a new tricritical point, other independent approaches will be more than welcome. Our enumerations have large error bars, due mostly to the uncertainty in the determination of the location of θ_t of the tricritical point. Other methods may give more precise values for the exponents. These include Monte Carlo simulations[16–18] of large clusters and finite-size scaling[19] (in 2D) which have in the past been proved to be the most efficient on similar problems. Recently exact values for the tricritical exponents at the Θ point were conjectured.[15] Since all 2D models are presumed to be conformal invariant at their critical (tricritical) points,[18] the same should hold for the one discussed here. We therefore urge this tricritical point to be located within the classification implied by the conformal invariance[18] which will yield the exact values of the 2D exponents.

ACKNOWLEDGMENTS

We are grateful to A. Aharony, S. Fishman, P.-G de Gennes, Y. Oono, P. Pincus, V. Privman, and M. Rubinstein for very fruitful discussions. This work was sup-

ported in part by funds provided by the Xerox Webster Research Center. We thank the High Energy Physics group at the University of Rochester for using their computer facilities during the early stage of the simulations. One of us (H.A.L.) would like to thank the Supercomputer Computations Research Institute staff and Miss D. E. Middleton for assistance and the partial support provided by the U. S. Department of Energy under the Contract No. DE-FC05-85ER250000.

---

*Permanent address: AT&T Bell Laboratories, 480 Red Hill Road, Middletown, New Jersey 07748.

[1]Y. Shapir and Y. Oono, J. Phys. A **17**, L39 (1984).
[2]H. A. Lim, A. Guha, and Y. Shapir, J. Phys. A **21**, 773 (1988).
[3]A. Guha, H. A. Lim, and Y. Shapir, J. Phys. A **21**, 1043 (1988).
[4]Y. Shapir, A. Guha, and H. A. Lim (unpublished).
[5]A. Malakis, J. Phys. A **9**, 1283 (1976).
[6]A. J. Guttmann, J. Phys. A **18**, 567 (1985); **18**, 575 (1985).
[7]P. J. Flory, *Principles of Polymer Chemistry* (Cornell University Press, Ithaca, 1953).
[8]P. G. de Gennes, *Scaling Concepts in Polymer Physics* (Cornell University Press, Ithaca, 1979).
[9]M. Stephen, Phys. Lett. **53A**, 363 (1975).
[10]M. A. Moore, J. Phys. A **10**, 305 (1977).
[11]Y. Oono and T. Oyama, J. Phys. Soc. Jpn. **49**, 301 (1978).
[12]D. C. Rapaport, J. Phys. A **10**, 637 (1977).
[13]T. Ishinabe, J. Phys. A **18**, 3181 (1985).
[14]V. Privman, J. Phys. A **19**, 3287 (1986).
[15]B. Duplantier and H. Saleur, Phys. Rev. Lett. **59**, 539 (1987).
[16]P. Lam, Phys. Rev. B **36**, 6988 (1987).
[17]H. Meirovitch and H. A. Lim, Phys. Rev. A **38**, 1670 (1988).
[18]J. Cardy, in *Phase Transitions and Critical Phenomena,* edited by C. Domb and J. L. Lebowitz (Academic, New York, 1987), Vol. XI.
[19]B. Derrida and H. J. Herrmann, J. Phys. (Paris) **44**, 1365 (1983).